INVERSION OF GRAVITY AND MAGNETIC FIELD DATA FOR TYRRHENA PATERA. C. Milbury[1], G. Schubert[1,2] C. A. Raymond[3], and S. E. Smrekar[3], [1]UCLA, Department of Earth and Space Sciences, 595 Charles Young Drive East, Los Angeles, CA 90095-1567 (cmilbury@ucla.edu), [2]Institute of Geophysics and Planetary Physics, UCLA, Los Angeles, CA 90095-1567, [3]Jet Propulsion Laboratory, California Institute of Technology, Pasadena, CA 91109.

Introduction: Tyrrhena Patera is located to the southeast/northeast of the Isidis/Hellas impact basin. It was geologically active into the Late Amazonian, although the main edifice was formed in the Noachian (~3.7-4.0 Ga) [1]. Tyrrhena Patera and the surrounding area contain gravity and magnetic anomalies that appear to be correlated (see Fig. 1). The results presented here are for the anomalies 1a and 1b (closest to Tyrrhena Patera), however other anomalies in this region have been modeled and will be presented at the conference.

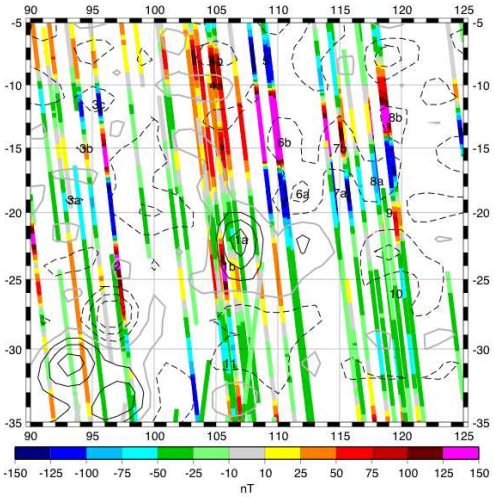

Fig. 1. Radial component of the magnetic field (nT) with 50 mgal contours of the isostatic gravity for a 40 km thick layer. Solid lines are positive, dashed lines are negative and grey is the zero line. The numbers indicate locations of modeled magnetic anomalies.

The Mars Global Surveyor (MGS) free-air gravity signature of Tyrrhena Patera has been studied by [2], who inferred the existence of an extinct magma chamber below it. The magnetic signature has been mapped by [3], who compared electron reflectometer data, analogous to the total magnetic field, for Syrtis Major and Tyrrhena Patera and argued for demagnetization of both volcanoes.

Data: Free-air gravity and topography data used are specified on 1º Cartesian grids derived from the spherical harmonic gravity model MRO110B2 [4] and the MOLA topography [5]. The Bouguer and isostatic gravity anomalies are calculated to examine the spatial variability in the subsurface structure.

The full resolution available in the 3-component magnetic measurements of MGS acquired during the AeroBraking (AB) and nighttime Science Phase Orbit (SPO) phases of the mission at altitudes less than Mapping Orbit (MO) Phase altitudes (400 km) are used. The maximum of the radial component of the magnetic field (~50 nT) is located near the caldera of Tyrrhena Patera (106.2º E, -21.4º N) at ~200 km altitude.

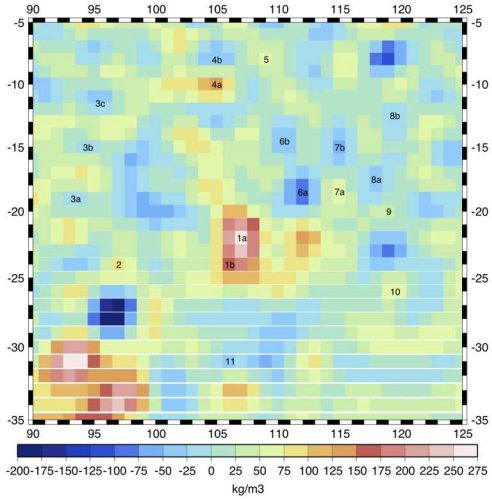

Fig. 2. Predicted density for the best-fit layer with a depth/thickness of 0/25 km. Numbers indicate the locations of the modeled magnetic sources.

Methods: The data are inverted for the entire area shown in Figs. 1 and 2. The gravity data are inverted first since the observed gravity anomalies do not have the same horizontal ambiguity that the unknown paleopole introduces into the position of the magnetic anomalies, thereby giving better constrained results in the horizontal dimension. Sources are represented as a uniform mesh of square prisms that are 1º on each side, similar to the distribution of gravity data. The isostatic anomaly is inverted for a range of depth and thickness values (0-100 km) in increments of 5 km. The best-fit depth and thickness that minimize the least squares difference between the observed and predicted gravity are determined.

Magnetic sources are represented as prisms with square cross-sections and are placed according to the following: 1) where there is a density anomaly, 2) where magnetic field data coverage is good, and, 3) where the magnetic field is strong (see Figs. 1 and 2). The depth, thickness, horizontal extent and location of the magnetic sources are determined by the gravity inversion. The magnetic field data are inverted over an

array of paleopole positions in order to find the best-fit paleopole position that minimizes the root mean square (rms) difference between the observed and predicted magnetic fields. Anomalies 1a and 1b are inverted separately, and together.

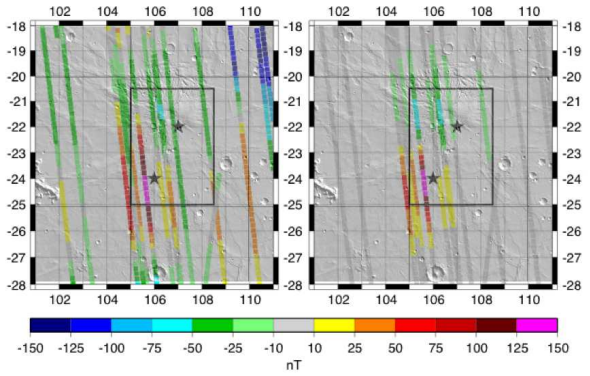

Fig. 3. Radial component of the observed (left) and predicted (right) magnetic field with shaded MOLA topography for Tyrrhena Patera. Stars indicate magnetic source locations and the box indicates the area over which the rms difference is calculated.

Results and Conclusions: The gravity inversion gives a best-fit depth and thickness of 0 and 25 km, respectively. The predicted densities for the region are shown in Fig. 2. The location of anomaly 1a is selected to be at the maximum density location (107º E, -22º N) and anomaly 1b is at (106º E, -24º N).

When 1a and 1b are inverted together, the best-fit pole is located at (350º E, 15º N) and the magnitudes of the magnetization for anomalies 1a/1b are 23/-58 A/m. The magnetic field data and predicted magnetic field for this pole are shown in Fig. 3. When anomaly 1a is inverted alone, the best-fit poles/antipodes are located slightly to the north/south of the equator and the poles are not well constrained in latitude and longitude, most likely due to the small magnitude of the magnetic field (Fig. 4). Inversion of anomaly 1b alone, which is a stronger magnetic anomaly than 1a, yields best-fit poles/antipodes that are well constrained and centered near the equator on the 0/180º meridians (Fig. 4). Fig. 4 shows that the best-fit paleopole positions for the inversions of anomalies 1a and 1b are in good agreement with the results of inversions of isolated magnetic data, and with Milbury and Schubert [6] who found paleopoles by modeling of Mars' global magnetization. Perron et al. [7] determine a true polar wander path of Mars' rotational axis for the Arabia (~4 Ga) and Deuteronilus (~2 Ga) shoreline contacts to be along the 335º meridian, close to the best-fit pole for the combined inversion (350º E, 15º N). This supports the case for true polar wander along the path suggested by Perron et al. [7].

The magnetic signatures of these anomalies suggest a number of different magnetization scenarios. It's clear that 1a is magnetically weak compared to 1b. This could mean that the magmatism associated with Tyrrhena demagnetized the crust, as suggested by [3]. However, given its geologic age (~3.7-4 Ga [1]), it is possible that Tyrrhena acquired its magnetization while the dynamo was still active. It also implies that the bulk of the surrounding crust (and therefore 1b) could have been magnetized when the pole was oriented in the reversed position and 1a was magnetized at a later stage in the dynamo evolution when the strength was waning. Another possibility is that 1a acquired it's magnetization from 1b, which is ~200 km away.

The other anomalies shown in Figs. 1 and 2 have best-fit paleopoles that fall into two general categories: low latitude poles similar to those shown in Figure 4, and high latitude poles. Low latitude poles are favored by anomalies in the western and smoothed part of the study region (2, 3a, 3b, 3c, 4a, 5, 6b, and 7b). High latitude paleopoles are favored by anomalies that are located in the eastern and cratered terrain (4b, 6a, 7a, 8a, 8b, 9, 10 and 11.) The low latitude poles likely predate or occur within the period of true polar wander while the high latitude poles postdate this period.

References: [1] Williams D. A. et al. (2008) *JGR*, *113*, doi:10.1029/2008JE003104. [2] Kiefer W. S. (2003) *6th Int. Conf. on Mars,* Abstract # 3252. [3] Lillis R. J. et al. (2008) *Icarus, 194,* 575-596. [4] Konopliv A.S. et al. (2010) *Icarus,* doi:10.1016/ j.icarus.2010.10.004. [5] Zuber M. T. et al (2000) *Science, 287,* 1788-1793. [6] Milbury C. and Schubert G. (2010) *JGR, 115*, doi:10.1029/2010JE003617. [7] Perron J. T. et al (2007) *Nature, 447,* 840-843.

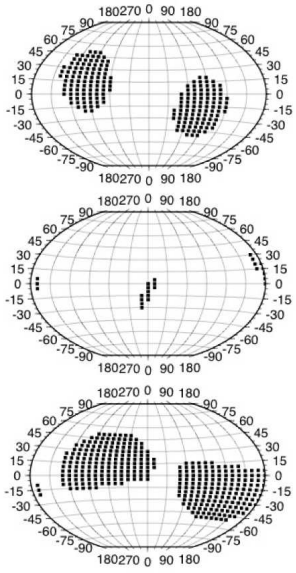

Figure 4. Best-fit paleopole positions determined by the inversions of 1a (top), 1b (middle) and joint 1a/b (bottom). They're found using the equation: 0.1* (rms_{max}-rms_{min})+rms_{min}, where rms is the rms difference between the radial component of the observed and predicted magnetic field.